

Hierarchical Tubular Structures Composed of Co₃O₄ Hollow Nanoparticles and Carbon Nanotubes for Lithium Storage

Chen, Yu Ming; Yu, Le; Lou, Xiong Wen David

2016

Chen, Y. M., Yu, L., & Lou, X. W. D. (2016). Hierarchical Tubular Structures Composed of Co₃O₄ Hollow Nanoparticles and Carbon Nanotubes for Lithium Storage. *Angewandte Chemie International Edition*, 55, 5990–5993.

<https://hdl.handle.net/10356/80621>

<https://doi.org/10.1002/anie.201600133>

© 2016 Wiley-VCH Verlag GmbH & Co. KGaA, Weinheim. This is the author created version of a work that has been peer reviewed and accepted for publication by *Angewandte Chemie International Edition*, Wiley-VCH Verlag GmbH & Co. KGaA, Weinheim. It incorporates referee's comments but changes resulting from the publishing process, such as copyediting, structural formatting, may not be reflected in this document. The published version is available at: [<http://dx.doi.org/10.1002/anie.201600133>].

Downloaded on 25 Aug 2022 21:21:01 SGT

Hierarchical Tubular Structures Composed of Co₃O₄ Hollow Nanoparticles and Carbon Nanotubes for Lithium Storage

Yu Ming Chen, Le Yu, and Xiong Wen (David) Lou*

[*] Dr. Y. M. Chen, L. Yu, Prof. X. W. Lou

School of Chemical and Biomedical Engineering, Nanyang Technological University, 62 Nanyang Drive, Singapore 637459, Singapore

Email: xwlou@ntu.edu.sg

Webpage: <http://www.ntu.edu.sg/home/xwlou/>

Abstract

Hierarchical tubular structures composed of Co₃O₄ hollow nanoparticles and carbon nanotubes (CNTs) have been synthesized by an efficient multi-step route. Starting from polymer-cobalt acetate (Co(Ac)₂) composite nanofibers, uniform polymer-Co(Ac)₂@zeolitic imidazolate framework-67 (ZIF-67) core-shell nanofibers are first synthesized via partial phase transformation with 2-methylimidazole in ethanol. After the dissolution of polymer-Co(Ac)₂ cores in an organic solvent, the resulting ZIF-67 tubular structures can be converted into hierarchical CNTs/Co-carbon hybrids by annealing in Ar/H₂ atmosphere. Finally, the hierarchical CNT/Co₃O₄ microtubes are obtained by a subsequent thermal treatment in air. Impressively, the as-prepared nanocomposite delivers a high reversible capacity of ~1281 mAh g⁻¹ at 0.1 A g⁻¹ with exceptional rate capability and long cycle life over 200 cycles when evaluated as an anode material for lithium-ion batteries.

Key words: Co₃O₄, ZIF-67, hierarchical microtubes, hollow nanoparticles, lithium-ion batteries.

Lithium-ion batteries (LIBs) have been the focus of intensive efforts for portable electronic devices, electric vehicles, and hybrid electric vehicles.^[1-6] However, existing commercial graphite based anodes have a relatively low theoretical capacity of 372 mAh g⁻¹, which is far below the specifications required in large-scale energy applications.^[7-9] Thus, it is highly desirable to explore alternative anode materials that could endow LIBs with higher energy density and better rate performance. As a typical family of transition metal oxides (TMOs), Cobalt oxide based materials have attracted a lot of attention as promising anode materials.^[10-13] Of particular note, mixed-valent Co₃O₄ can theoretically deliver as high as three times the capacity of graphite due to its 8-electron transfer reaction upon cycling.^[13-19] Unfortunately, the practical applications of Co₃O₄-based electrodes are largely hampered due to the poor electrical conductivity and the large volumetric variation during the charging-discharging processes.^[12-13, 20-21]

Nanostructured electrode materials can enhance the electrochemical performance that could not be achieved in traditional bulk materials, benefiting from the higher surface area and shorter diffusion path.^[22-25] Amongst various structural designs, considerable attention has been paid to hierarchical tubular structures (HTSs) for electrochemical energy storage in view of their many advantages such as enlarged electrode/electrolyte contact area and pore volume. These hierarchical microtubes are usually organized by low-dimensional building blocks. For instance, Wang and co-workers reported a simple solution-phase method for constructing robust tubular structure composed of single-layered MoS₂ with greatly enhanced capacity and excellent cycling performance for lithium storage.^[26] Our group has also synthesized several hierarchical tubulars constructed from Mn-based mixed metal oxide nanoflakes and TiO₂ (B) nanosheets by an efficient template-based strategy along with different post treatments as advanced electrode materials.^[27-28] More recently, great efforts have been devoted to designing hybrid nanostructures of inorganic nanostructures and carbon-based species for LIBs application. It is generally believed that these hybrid constructions could simultaneously overcome the shortcomings of poor mechanical stability

and poor electrical conductivity in simple inorganic materials.^[29-32] Therefore, it is interesting to incorporate carbonaceous materials into TMO-based HTSs. Despite the progresses mentioned above, the designed synthesis of HTSs constructed from different types of functional subunits is still quite challenging due to the limitations of synthetic strategies.

Herein, we have designed a multi-step strategy for the efficient synthesis of novel HTSs composed of Co_3O_4 hollow nanoparticles and carbon nanotubes (CNTs). Through a controlled chemical transformation process, zeolitic imidazolate framework-67 (ZIF-67) tubulars have been made as the single source for carbon and cobalt in the final composite. After a two-step annealing treatment, the hierarchical CNT/ Co_3O_4 microtubes are obtained, which inherit unique structural features from the different functional subunits. Specifically, these HTSs constructed by hollow nanoparticles can provide sufficient active interfacial sites and effectively alleviate the volume variation during the electrochemical reactions. The well-distributed CNTs on the HTSs ensure the enhanced electron transfer and prevent the aggregation of Co_3O_4 nanoparticles during repeated discharging/charging cycling processes. As expected, the as-prepared hierarchical CNT/ Co_3O_4 microtubes show excellent electrochemical properties when evaluated as an anode material for LIBs.

The synthesis process of the hierarchical CNT/ Co_3O_4 microtubes involves the following steps as schematically shown in **Figure 1** (for experimental details, see Supporting Information). Electrospun polyacrylonitrile (PAN)-cobalt acetate ($\text{Co}(\text{Ac})_2$) composite nanofibers are selected as the self-engaged templates to provide the cobalt source for the growth of ZIF-67. Next, due to the strong coordination of 2-methylimidazole to cobalt ions within the PAN- $\text{Co}(\text{Ac})_2$ nanofibers, a uniform shell of ZIF-67 nanocrystals can be grown on the nanofibers. After being dispersed in *N,N*-dimethylformamide (DMF) to dissolve the PAN- $\text{Co}(\text{Ac})_2$ core, the obtained ZIF-67 tubulars can be further converted into CNT/Co-carbon hybrids through a heating treatment in Ar/H_2 . During this process, elemental Co nanoparticles are first yielded in the strong reduction atmosphere. At the same time, the highly dispersed Co nanoparticles can catalyze the growth of CNTs from carbon

precursor,^[33-35] leading to the formation of the hierarchical hybrids. Finally, these Co nanoparticles are oxidized to Co₃O₄ hollow nanoparticles via a thermal annealing in air while the CNTs can be well retained, generating hierarchical CNT/Co₃O₄ microtubes.

Co(Ac)₂ can be uniformly distributed in the PAN nanofibers to form the PAN-Co(Ac)₂ composite nanofibers with a diameter of 150 ± 50 nm by an electrospinning method (Figure S1a-c, see Supporting Information), as confirmed by energy-dispersive spectroscopy (EDX) spectrum (Figure S1d, see Supporting Information). The typical field-emission scanning electron microscopy (FESEM) images (Figure S2a-c, see Supporting Information) show that 2-methylimidazole can react with Co(Ac)₂ in the composite nanofibers to generate ZIF-67 nanocrystals. Transmission electron microscopy (TEM) images clearly reveal a core-shell structure (Figure S2d-f, see Supporting Information). XRD pattern of the composites indicates typical diffraction peaks of ZIF-67 phase (Figure S3a, see Supporting Information).^[36-37] As elucidated in **Figure 2**, the PAN-Co(Ac)₂ core is completely removed after the treatment in DMF. The remaining ZIF-67 nanocrystals are interconnected to build tubular structures with lengths up to several micrometers. In addition, the ZIF-67 particle size is about 40 to 80 nm, which can be slightly reduced using methanol as the solvent (Figure S4, see Supporting Information). When annealed in Ar/H₂ atmosphere, the as-synthesized ZIF-67 microtubes can be transformed into the CNT/Co-carbon hybrids. Some multi-walled CNTs can be clearly identified on the surface of Co-carbon composite (Figure S5, see Supporting Information). The interplanar spacings of 0.34 nm and 0.21 nm correspond to the (002) planes of carbon and the (111) planes of Co, respectively. Selected area electron diffraction (SAED) pattern (Figure S5c, see Supporting Information) and XRD pattern (Figure S3b, see Supporting Information) further confirm the presence of elemental Co.

In the final step, a mild annealing treatment at 360 °C in air is employed to convert the CNT/Co-carbon composites into the hierarchical CNT/Co₃O₄ microtubes. The tubular morphology of the materials is well maintained after the oxidation process (**Figure 3**, and Figure S6 in the Supporting

Information). More interestingly, the tubulars are mainly organized by Co_3O_4 hollow nanoparticles with a size ranged from 15 to 30 nm (Figure 3c-e). The transformation from Co solid nanoparticles into Co_3O_4 hollow particles can be attributed to the Kirkendall effect during the annealing process.^[38-39] Moreover, CNTs can be generally retained after the calcination in air, yielding hierarchical CNT/ Co_3O_4 microtubes (Figure 3b, d). In addition, the inner diameter of Co_3O_4 hollow nanoparticle and CNTs is about 10 ± 5 nm and 3 ± 2 nm, respectively (Figure 3d-f). The clear lattice fringes with an interplanar distance of 0.24 nm can be ascribed to the (311) planes of the cubic Co_3O_4 (Figure 3e). The crystallographic structure of the microtubes are then investigated by XRD (Figure S3b, see Supporting Information). All the diffraction peaks can be perfectly indexed to cubic Co_3O_4 (JCPDS card No.: 42-1467), which is consistent with the high-resolution TEM (HRTEM) image and selected area electron diffraction (SAED) analysis (Figure 3f and Figure S6c in the Supporting Information). EDX analysis reveals that the Co/O atomic ratio of the microtubes is about 0.79, which is close to the theoretical composition of Co_3O_4 (Figure S7, see Supporting Information). As verified by thermogravimetric analysis (TGA; Figure S8, see Supporting Information), the carbon content in the composite is ~13 %. The X-ray photoelectron spectroscopy (XPS) spectrum confirms the existence of pyridinic N (398.5 eV) and pyrrolic N (400.8 eV) in the composites (Figure S9, see Supporting Information). Moreover, the hierarchical CNT/ Co_3O_4 microtubes exhibit a high specific Brunauer-Emmett-Teller (BET) surface area of $93.9 \text{ m}^2 \text{ g}^{-1}$ with the pore sizes mostly below 15 nm (Figure S10, see Supporting Information). It is worth to mention that the selection of the calcination atmosphere and temperature in the two-step annealing treatment plays important roles in the generation of the unique hierarchical structures. If Ar is chosen rather than Ar/H_2 in the first-step of annealing treatment, only Co_3O_4 microtubes could be achieved without the formation of CNTs (Figure S11, see Supporting Information). When a lower calcining temperature is applied in the oxidization step, significant amount of residual carbon will remain in the final materials (Figure S7b and S12, see Supporting Information).

We next carry out the electrochemical evaluation of the hierarchical CNT/Co₃O₄ microtubes as an anode material for LIBs. Figure 4a presents the typical galvanostatic charge-discharge voltage profiles of the hierarchical microtubes at the current density of 0.1 A g⁻¹ within a cut-off voltage window of 0-3 V versus Li/Li⁺. A long voltage plateau at around 1.03 V and the other inconspicuous plateau at about 1.3 V can be observed in the first discharge process, corresponding to the reduction reactions of CoO to Co and Co₃O₄ to CoO, respectively.^[40] The main plateau at ~2.1 V can be assigned to the delithiation of Co to Co₃O₄ in the first charge process.^[16] The voltage plateau obviously shifts to about 1.25 V in the second discharge cycle, which could be mainly attributed to the structural variation of the electrode materials.^[20, 40] Nevertheless, the voltage profiles are well overlapping except for the initial discharge, indicating the good stability of the composites for reversible lithium storage. The representative cyclic voltammetry (CV) curves of these hierarchical microtubes are well consistent with the above charge-discharge voltage profiles, further confirms the typical multi-step electrochemical processes of Co₃O₄ (Figure S13, see Supporting Information). The first charge and discharge specific capacities are about 1281 and 1840 mAh g⁻¹, respectively, which are much higher than those of the CNTs derived from the hierarchical CNT/Co₃O₄ microtubes after acid treatment (Figure S14, see Supporting Information). The relatively large irreversible capacity could be due to the formation of the solid-electrolyte interface (SEI) film and the decomposition of electrolyte.^[14, 17, 41]

The rate capability of the CNT/Co₃O₄ electrode is shown in Figure 4b. At current densities of 0.75, 1.25, 2, 2.5, and 3 A g⁻¹, the reversible capacities of the hierarchical microtubes are around 832, 768, 715, 673, and 643 mAh g⁻¹, respectively. Even at a relatively high current density of 6 A g⁻¹, the hierarchical hybrid can still deliver a capacity as high as 515 mAh g⁻¹, suggesting excellent high-rate capability. The capacity is slightly increased during the cycling process when the current density is decreased to 0.75 A g⁻¹, due to the reactivation process caused by the high-rate lithiation.^[42] More importantly, the hierarchical CNT/Co₃O₄ electrode also exhibits exceptional

cycling stability. As shown in Figure 4c, the as-prepared electrode shows a high capacity of 782 and 577 mAh g⁻¹ after 200 cycles at 1 and 4 A g⁻¹, respectively, without obvious capacity fading. The Coulombic efficiency (CE) for the CNT/Co₃O₄ composite electrode is close to 100 % after the first few cycles. This performance is superior to that of many other Co₃O₄-based anodes (Table S1, see Supporting Information). Post-mortem study shows that the shape and structural integrity of the CNT/Co₃O₄ composite can be well retained after 200 cycles (Figure S15, see Supporting Information). The outstanding performance of the hierarchical CNT/Co₃O₄ microtubes might be attributed to the unique structural and compositional features. To be specific, the construction of Co₃O₄ hollow nanoparticle and CNT subunits not only enables a short diffusion distance for fast diffusion of Li⁺ ions but also provides sufficient contact between active material and electrolyte for the rapid charge-transfer reaction.^[20] Moreover, the tubular structures and void space within the Co₃O₄ nanoparticles can effectively withstand large volume variation upon cycling, therefore maintaining structural integrity.^[40] In addition, the CNTs integrated in the hierarchical tubulars can enhance the electronic conductivity thus improving the rate capability,^[34, 43] and the electrochemical reactivity further improving the electrochemical property.^[34]

In summary, we have exploited a multi-step method for the effective synthesis of hierarchical tubular structures composed of Co₃O₄ hollow nanoparticles and carbon nanotubes (CNTs). Electrospun polyacrylonitrile (PAN)-cobalt acetate (Co(Ac)₂) composite nanofibers are used as the self-engaged bi-functional template. Through a facile chemical transformation process and subsequent removal of the core, tubular-like structures of ZIF-67 nanocrystals are obtained with lengths of up to several micrometers. A two-step annealing process is applied to convert these ZIF-67 tubulars into hierarchical CNT/Co₃O₄ microtubes. Benefiting from the unique structural and compositional advantages, the as-prepared hierarchical CNT/Co₃O₄ tubular structures show exceptional electrochemical performance with superior rate capability and long life span when evaluated as an anode material for lithium-ion batteries.

Acknowledgement

The authors are grateful to the Ministry of Education (Singapore) for financial support through the AcRF Tier 2 funding (MOE2014-T2-1-058, ARC41/14; M4020223.120).

References

- [1] M. Armand, J. M. Tarascon, *Nature* **2008**, *451*, 652.
- [2] K. S. Kang, Y. S. Meng, J. Breger, C. P. Grey, G. Ceder, *Science* **2006**, *311*, 977.
- [3] Y. Idota, T. Kubota, A. Matsufuji, Y. Maekawa, T. Miyasaka, *Science* **1997**, *276*, 1395.
- [4] A. Kushima, X. H. Liu, G. Zhu, Z. L. Wang, J. Y. Huang, J. Li, *Nano Lett.* **2011**, *11*, 4535.
- [5] H. Jiang, D. Ren, H. Wang, Y. Hu, S. Guo, H. Yuan, P. Hu, L. Zhang, C. Li, *Adv. Mater.* **2015**, *27*, 3687.
- [6] H. Geng, Q. Zhou, Y. Pan, H. Gu, J. Zheng, *Nanoscale* **2014**, *6*, 3889.
- [7] Y. Chen, Z. Lu, L. Zhou, Y.-W. Mai, H. Huang, *Energy Environ. Sci.* **2012**, *5*, 7898.
- [8] K. Sato, M. Noguchi, A. Demachi, N. Oki, M. Endo, *Science* **1994**, *264*, 556.
- [9] Z.-J. Fan, J. Yan, T. Wei, G.-Q. Ning, L.-J. Zhi, J.-C. Liu, D.-X. Cao, G.-L. Wang, F. Wei, *ACS Nano* **2011**, *5*, 2787.
- [10] Y. Sun, X. Hu, W. Luo, Y. Huang, *J. Phys. Chem. C* **2012**, *116*, 20794.
- [11] X. Guan, J. Nai, Y. Zhang, P. Wang, J. Yang, L. Zheng, J. Zhang, L. Guo, *Chem. Mater.* **2014**, *26*, 5958.
- [12] D. Gu, W. Li, F. Wang, H. Bongard, B. Spliethoff, W. Schmidt, C. Weidenthaler, Y. Xia, D. Zhao, F. Schüth, *Angew. Chem., Int. Ed.* **2015**, *54*, 7060.
- [13] J. Wang, N. Yang, H. Tang, Z. Dong, Q. Jin, M. Yang, D. Kisailus, H. Zhao, Z. Tang, D. Wang, *Angew. Chem., Int. Ed.* **2013**, *52*, 6417.
- [14] R. Tummala, R. K. Guduru, P. S. Mohanty, *J. Power Sources* **2012**, *199*, 270.
- [15] W. Wen, J. M. Wu, M. H. Cao, *Nanoscale* **2014**, *6*, 12476.
- [16] X. Yang, K. Fan, Y. Zhu, J. Shen, X. Jiang, P. Zhao, S. Luan, C. Li, *ACS Appl. Mater. Interfaces* **2013**, *5*, 997.
- [17] Z. S. Wu, W. Ren, L. Wen, L. Gao, J. Zhao, Z. Chen, G. Zhou, F. Li, H. M. Cheng, *ACS Nano* **2010**, *4*, 3187.
- [18] D. Qiu, G. Bu, B. Zhao, Z. Lin, L. Pu, L. Pan, Y. Shi, *Mater. Lett.* **2014**, *119*, 12.
- [19] B. Wang, X. Y. Lu, Y. Y. Tang, *J. Mater. Chem. A* **2015**, *3*, 9689.
- [20] S. Abouali, M. Akbari Garakani, B. Zhang, H. Luo, Z.-L. Xu, J.-Q. Huang, J. Huang, J.-K. Kim, *J. Mater. Chem. A* **2014**, *2*, 16939.
- [21] H. Geng, H. Ang, X. Ding, H. Tan, G. Guo, G. Qu, Y. Yang, J. Zheng, Q. Yan, H. Gu, *Nanoscale* **2016**, *8*, 2967.
- [22] M. V. Reddy, G. V. Subba Rao, B. V. R. Chowdari, *Chem. Rev.* **2013**, *113*, 5364.
- [23] X. Y. Yu, L. Yu, X. W. Lou, *Adv. Energy Mater.* **2016**, *6*, 1501333.

- [24] S. Goriparti, E. Miele, F. De Angelis, E. Di Fabrizio, R. Proietti Zaccaria, C. Capiglia, *J. Power Sources* **2014**, 257, 421.
- [25] L. Ji, Z. Lin, M. Alcoutlabi, X. Zhang, *Energy Environ. Sci.* **2011**, 4, 2682.
- [26] P. P. Wang, H. Y. Sun, Y. J. Ji, W. H. Li, X. Wang, *Adv. Mater.* **2014**, 26, 964.
- [27] Y. Guo, L. Yu, C.-Y. Wang, Z. Lin, X. W. Lou, *Adv. Funct. Mater.* **2015**, 25, 5184.
- [28] H. Hu, L. Yu, X. Gao, Z. Lin, X. W. Lou, *Energy Environ. Sci.* **2015**, 8, 1480.
- [29] X. K. Huang, S. M. Cui, J. B. Chang, P. B. Hallac, C. R. Fell, Y. T. Luo, B. Metz, J. W. Jiang, P. T. Hurley, J. H. Chen, *Angew. Chem., Int. Ed.* **2015**, 54, 1490.
- [30] X. Y. Yu, H. Hu, Y. W. Wang, H. Y. Chen, X. W. Lou, *Angew. Chem., Int. Ed.* **2015**, 54, 7395.
- [31] G. Huang, F. F. Zhang, X. C. Du, Y. L. Qin, D. M. Yin, L. M. Wang, *ACS Nano* **2015**, 9, 1592.
- [32] H. L. Wang, H. J. Dai, *Chem. Soc. Rev.* **2013**, 42, 3088.
- [33] R. Wu, D. P. Wang, X. Rui, B. Liu, K. Zhou, A. W. K. Law, Q. Yan, J. Wei, Z. Chen, *Adv. Mater.* **2015**, 27, 3038.
- [34] Y. Chen, X. Li, K. Park, J. Song, J. Hong, L. Zhou, Y.-W. Mai, H. Huang, J. B. Goodenough, *J. Am. Chem. Soc.* **2013**, 135, 16280.
- [35] B. Y. Xia, Y. Yan, N. Li, H. B. Wu, X. W. Lou, X. Wang, *Nat. Energy* **2016**, 1, 15006.
- [36] H. Hu, B. Guan, B. Xia, X. W. Lou, *J. Am. Chem. Soc.* **2015**, 137, 5590.
- [37] H. Hu, L. Han, M. Z. Yu, Z. Wang, X. W. Lou, *Energy Environ. Sci.* **2016**, 9, 107.
- [38] F. Zhang, C. Yuan, J. Zhu, J. Wang, X. Zhang, X. W. Lou, *Adv. Funct. Mater.* **2013**, 23, 3909.
- [39] Y. D. Yin, R. M. Rioux, C. K. Erdonmez, S. Hughes, G. A. Somorjai, A. P. Alivisatos, *Science* **2004**, 304, 711.
- [40] G. Huang, F. Zhang, X. Du, Y. Qin, D. Yin, L. Wang, *ACS Nano* **2015**, 9, 1592.
- [41] W. Hao, S. Chen, Y. Cai, L. Zhang, Z. Li, S. Zhang, *J. Mater. Chem. A* **2014**, 2, 13801.
- [42] H. Sun, G. Xin, T. Hu, M. Yu, D. Shao, X. Sun, J. Lian, *Nat. Commun.* **2014**, 5, 4526.
- [43] L. Qie, W. M. Chen, Z. H. Wang, Q. G. Shao, X. Li, L. X. Yuan, X. L. Hu, W. X. Zhang, Y. H. Huang, *Adv. Mater.* **2012**, 24, 2047.

Figures and Captions

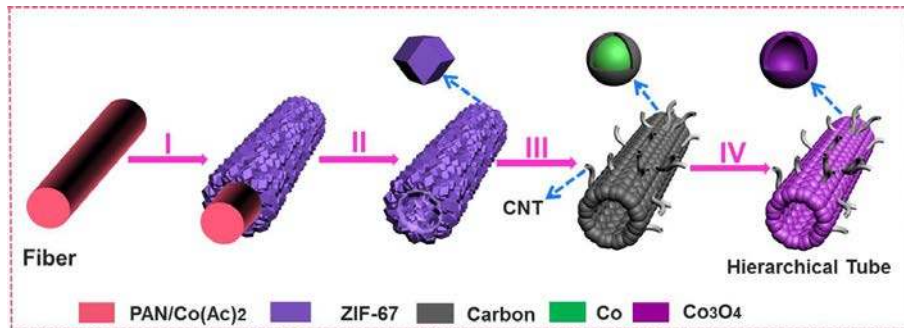


Figure 1. Schematic illustration of the formation of the hierarchical CNT/Co₃O₄ microtubes. (I) The growth of ZIF-67 onto the PAN-Co(Ac)₂ composite nanofiber. (II) Removal of the PAN-Co(Ac)₂ core. (III) Heating treatment in Ar/H₂ to convert ZIF-67 tubular structures to hierarchical CNT/Co-carbon composites. (IV) Further calcination in air to obtain hierarchical CNT/Co₃O₄ microtubes.

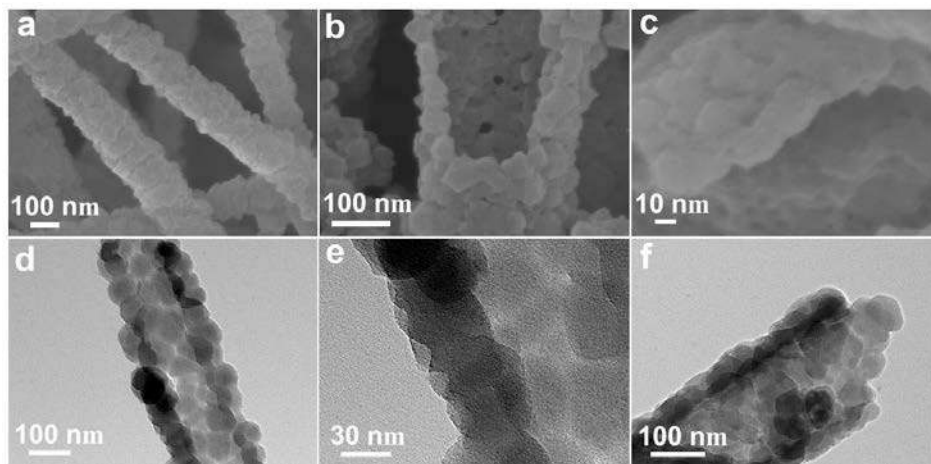


Figure 2. (a-c) FESEM and (d-f) TEM images of the synthesized ZIF-67 microtubes.

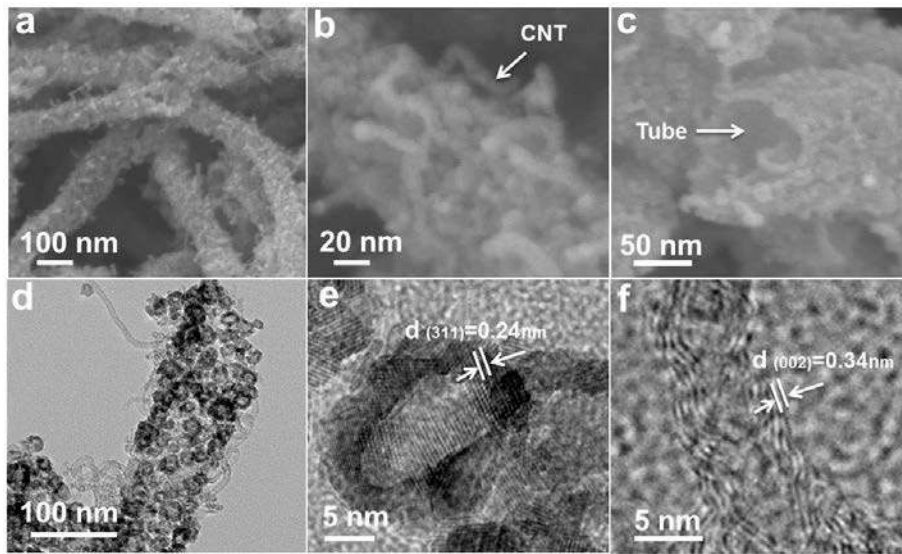


Figure 3. (a-c) FESEM, (d) TEM, and (e, f) HRTEM images of the synthesized hierarchical CNT/Co₃O₄ microtubes.

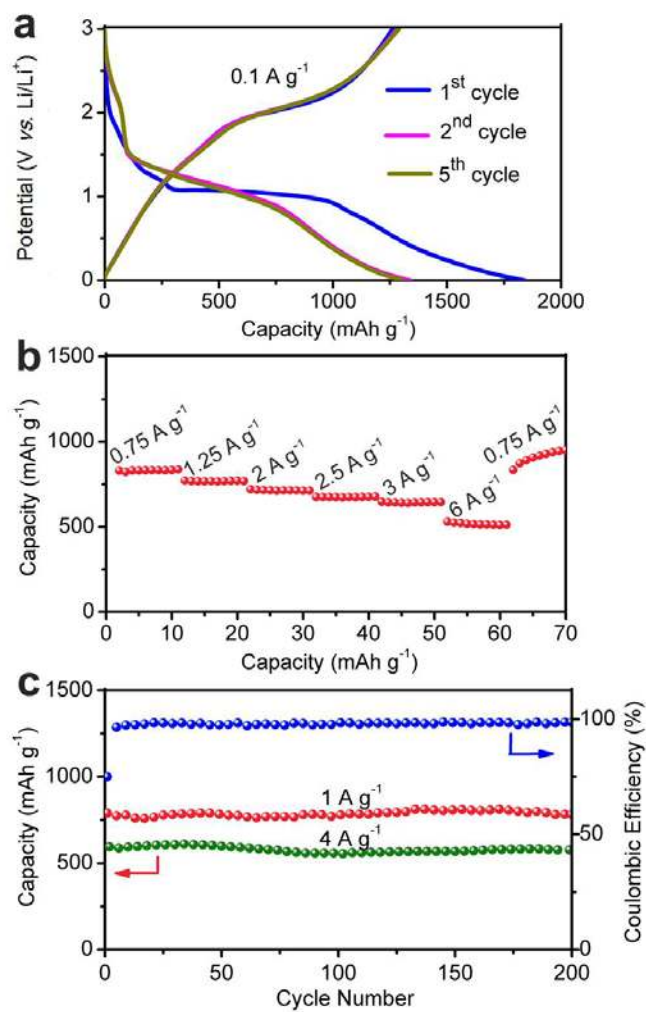
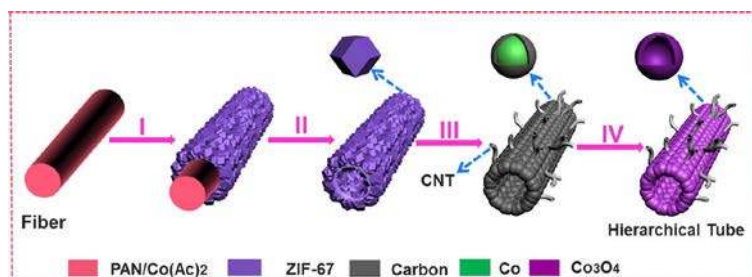


Figure 4. Electrochemical performance of the hierarchical CNT/Co₃O₄ microtubes. **(a)** Charge-discharge profiles at 0.1 A g⁻¹, **(b)** rate performance, and **(c)** cycling performance at 1 A g⁻¹ and 4 A g⁻¹.

For Table of Content Entry



Novel hierarchical tubular structures composed of Co₃O₄ hollow nanoparticles and carbon nanotubes are synthesized from the polymer/cobalt acetate composite nanofibers. Benefiting from unique structural and compositional features, the as-synthesized hierarchical tubular structures show excellent lithium storage properties.

Supporting Information

Experimental Section

Synthesis of the PAN-Co(Ac)₂ composite nanofibers. 1 g of polyacrylonitrile (PAN, Aldrich) was dissolved in 16 mL of dimethylformamide (DMF, Aldrich) solvent, followed by the addition of 3 g of cobalt acetate tetrahydrate (Aldrich) with vigorous stirring. The mixture solution of PAN-Co(Ac)₂ was loaded into a 20 mL syringe. The high voltage, feeding rate, and distance between the cathode and the anode were fixed at 16 kV, 0.05 mm min⁻¹, and 20 cm, respectively.

Synthesis of ZIF-67 microtubes. In a typical process, 12 mg of the prepared PAN-Co(Ac)₂ composite nanofibers was added into 10 mL of ethanol solution with 0.65 g of 2-methylimidazole (Aldrich) and then kept at room temperature for 24 h to obtain the core-shell PAN-Co(Ac)₂@ZIF-67 composite nanofibers. Then, the above core-shell composite nanofibers were dispersed in DMF at 50 °C with stirring to completely remove the PAN-Co(Ac)₂ core for generating the ZIF-67 microtubes.

Synthesis of the hierarchical CNT/Co₃O₄ microtubes. The as-synthesized ZIF-67 microtubes were first heated in Ar(95 %)/H₂(5 %) at 750 °C for 2 h with a heating rate of 2 °C min⁻¹ to obtain hierarchical CNT/Co-carbon hybrid, followed by a further thermal annealing in air at 360 °C for 10 min to obtain hierarchical CNT/Co₃O₄ microtubes.

Materials characterization. The prepared materials were analysed by X-ray diffraction (XRD Bruker D2 phaser), transmission electron microscopy (TEM; JEOL, JEM-2010), high-resolution TEM (HRTEM), energy-dispersive X-ray spectroscopy (EDX, Oxford), field-emission scanning electron microscopy (FESEM; JEOL-6700), thermogravimetric analysis (TGA, Pyris Diamond), and X-ray photoelectron spectroscopy (XPS, PHI5600). The nitrogen sorption measurement was conducted by Autosorb 6B at 77 K.

Electrochemical measurements. The anode electrode was prepared by mixing the above active hierarchical materials (70 wt.%), carbon black (20 wt.%), and poly(vinyl difluoride) (PVDF, 10 wt.%). **The mass loading of the prepared electrode material is about 1 mg cm⁻².** Two-electrode 2032 coin cells were assembled in Ar-filled glove box with lithium foil as the counter/reference electrode, LiPF₆ (1 M) in a 50:50 (w/w) mixture of ethylene carbonate and diethyl carbonate as the electrolyte, a Celgard 2400 membrane as the separator, and the mixed slurry on copper foil as the working electrode. The charge-discharge tests were performed on a battery tester (LAND 2001 CT) between 0 and 3 V at several current densities. Cyclic voltammetry (CV) tests were conducted with a CHI 660C electrochemical workstation.

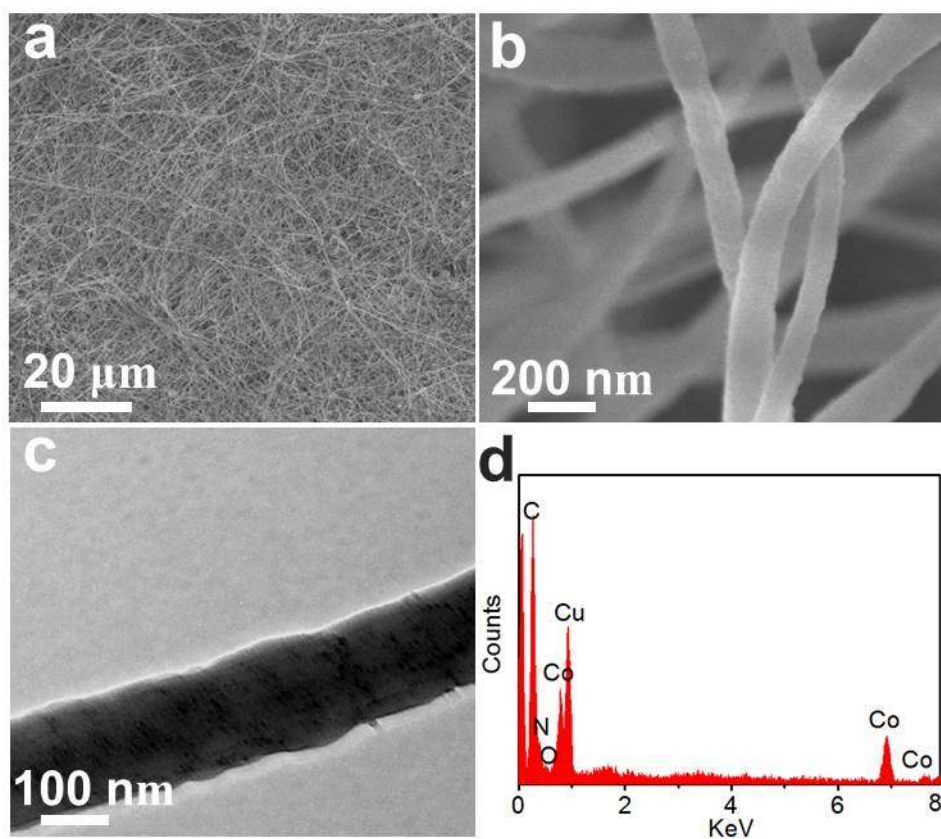


Figure S1. (a, b) FESEM and (c) TEM images and (d) EDX of the PAN-Co(Ac)₂ composite nanofibers. The peak of Cu in EDX is from the Cu substrate.

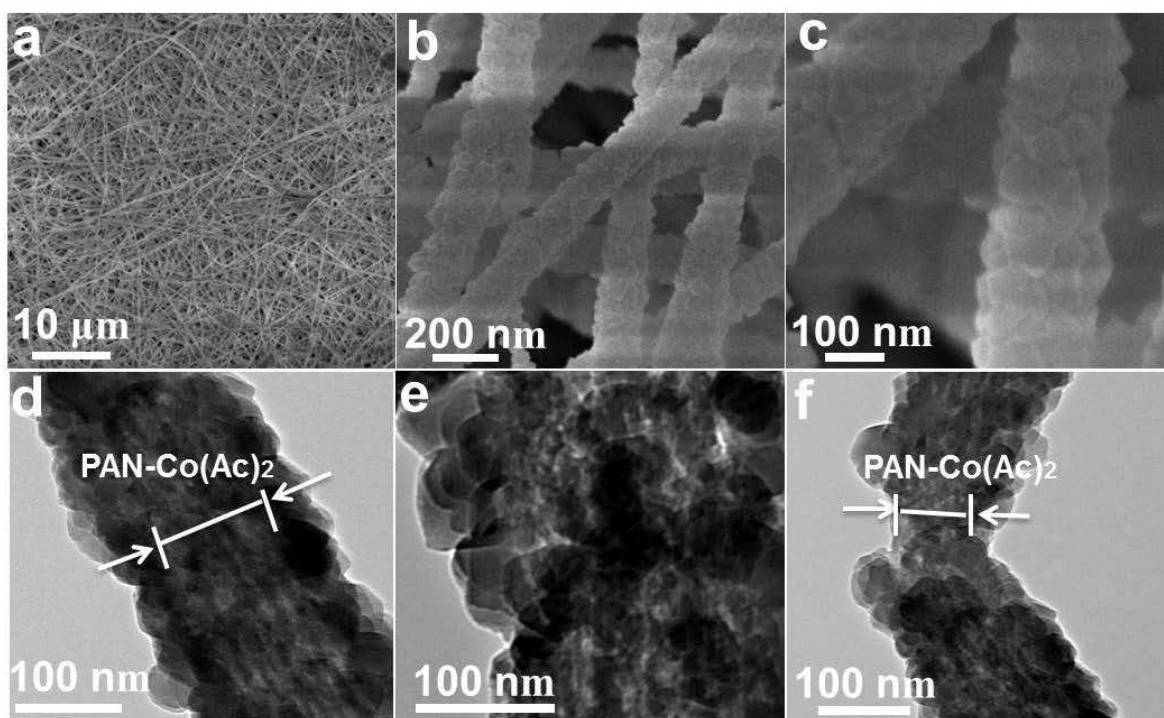


Figure S2. (a-c) FESEM and (d-f) TEM images of the core-shell PAN-Co(Ac)₂@ZIF-67 composite nanofibers.

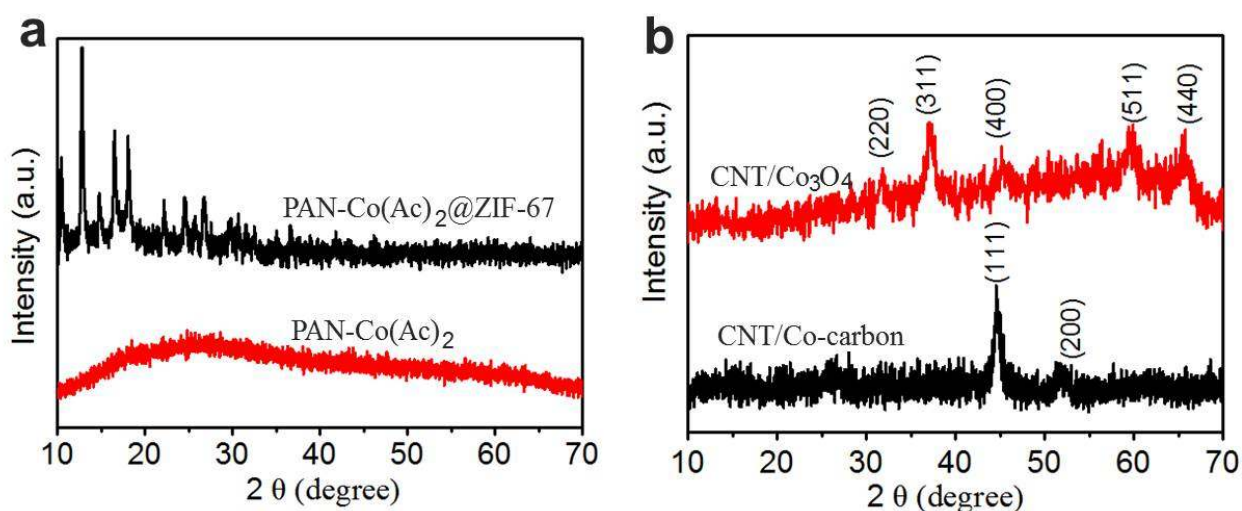


Figure S3. XRD patterns of (a) the PAN-Co(Ac)₂, PAN-Co(Ac)₂@ZIF-67, (b) hierarchical CNT/Co-carbon hybrid, and hierarchical CNT/Co₃O₄ microtubes.

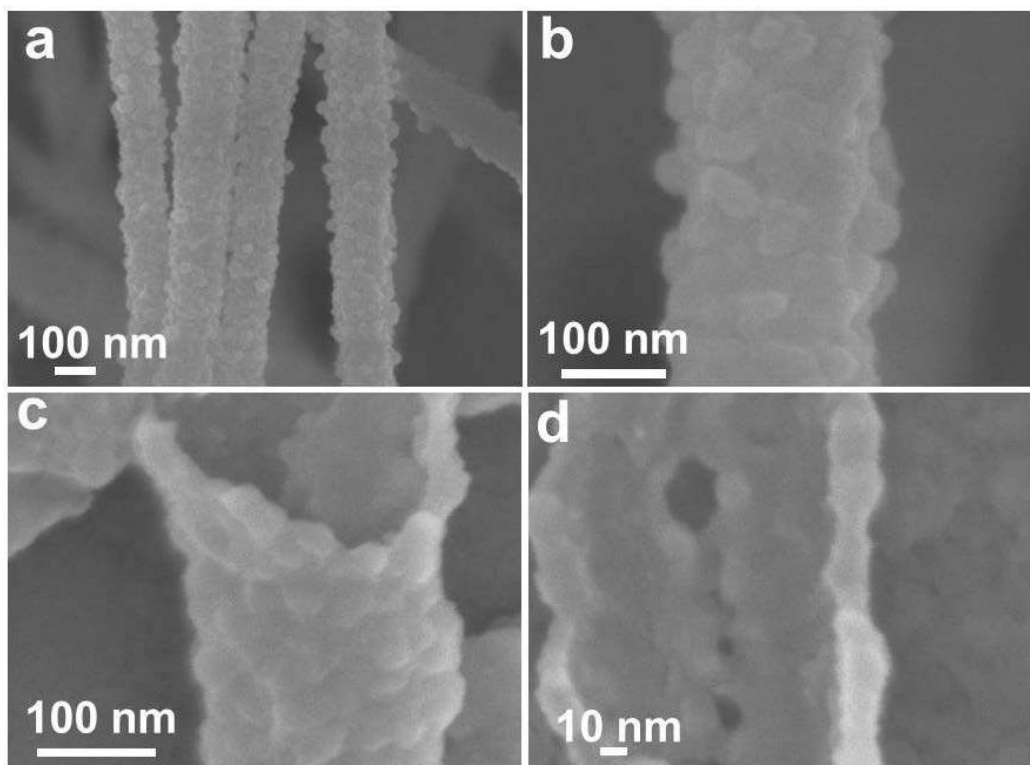


Figure S4. FESEM images of the synthesized ZIF-67 microtubes using methanol as the solvent.

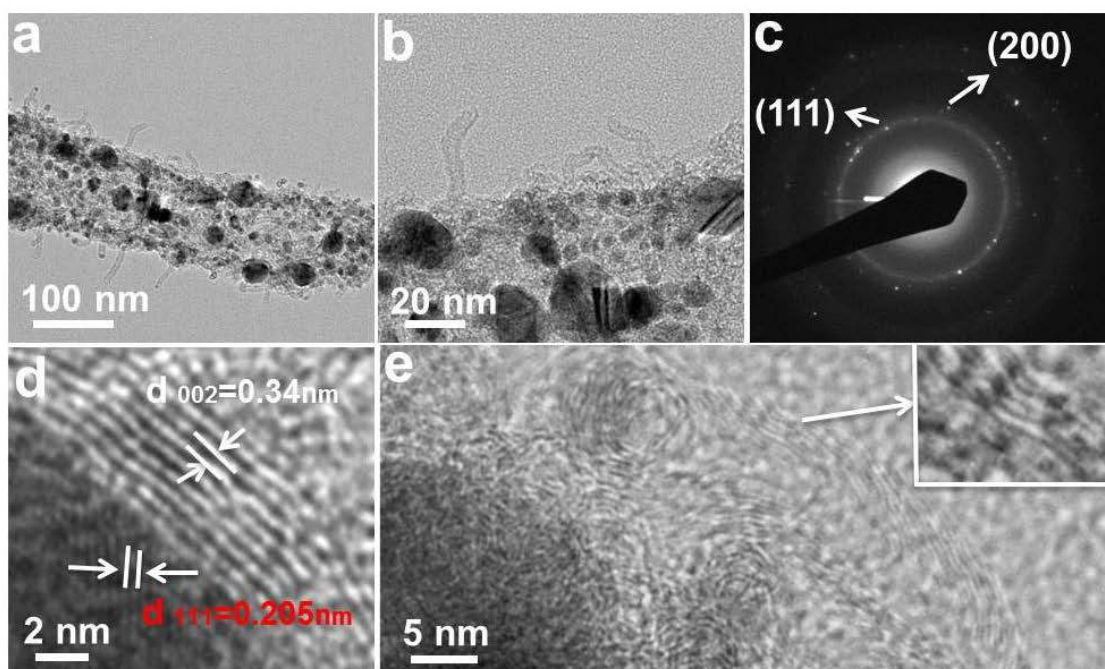


Figure S5. (a, b) TEM images (c) SAED pattern, and (d, e) HRTEM images of the synthesized hierarchical CNT/Co-carbon hybrid microtubes. The inset of (e) shows a magnified HRTEM image of an individual multi-wall CNT.

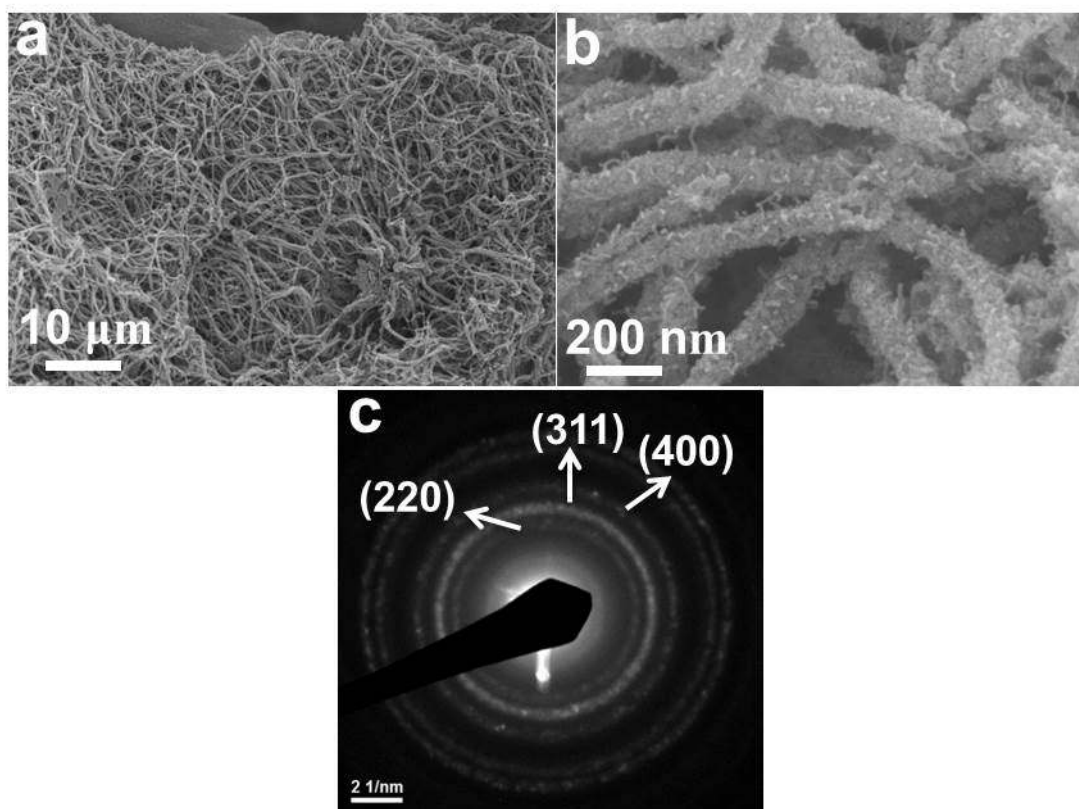


Figure S6. (a, b) FESEM images and (c) SAED pattern of the hierarchical CNT/Co₃O₄ microtubes.

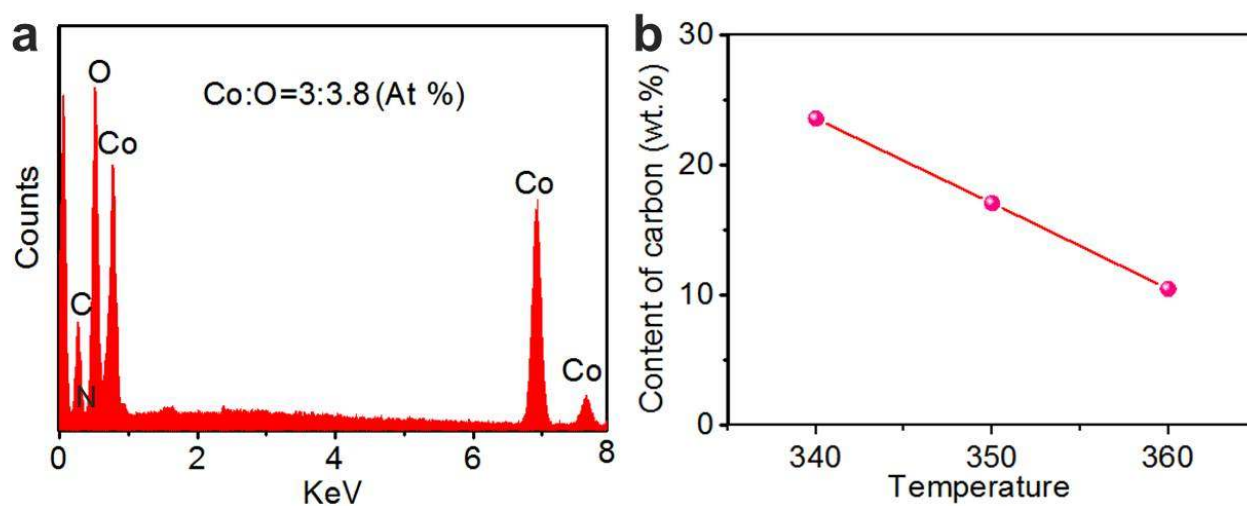


Figure S7. (a) EDX and (b) the content of carbon as a function of heating temperature of the synthesized hierarchical CNT/Co₃O₄ microtubes.

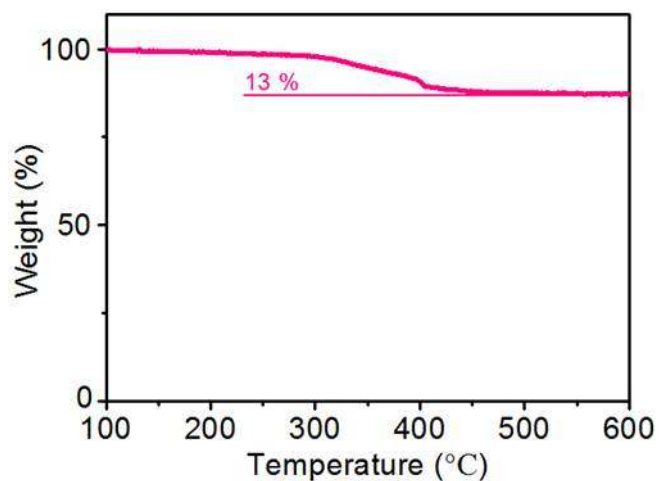


Figure S8. TGA curve of the synthesized hierarchical CNT/Co₃O₄ microtubes under air flow with a temperature ramp of 10 °C min⁻¹.

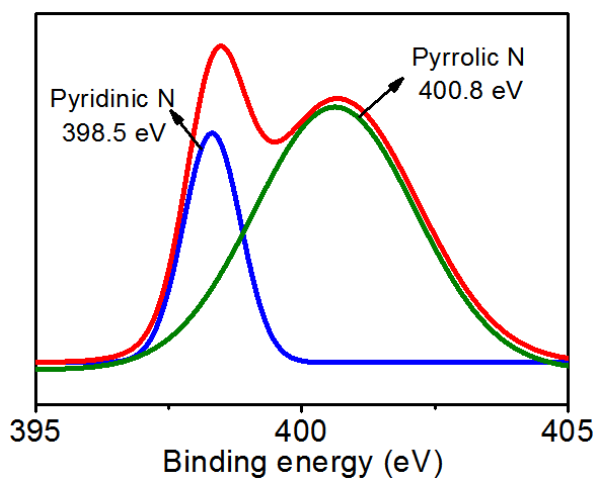


Figure S9. XPS spectrum of N1s. The fitted peaks can be assigned to pyridinic N (398.5 eV) and pyrrolic N (400.8 eV).

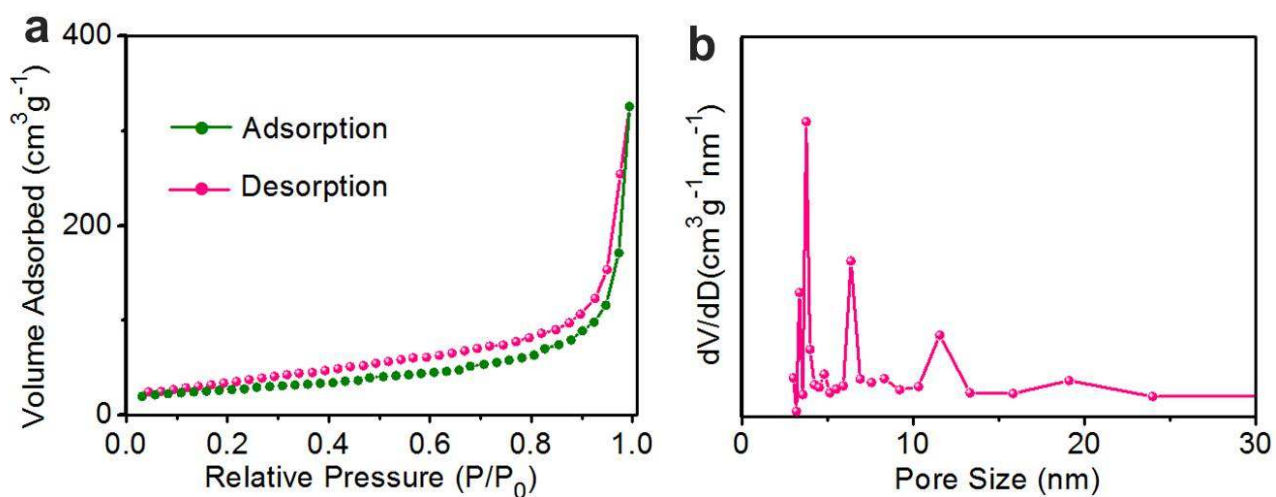


Figure S10. (a) N₂ adsorption-desorption isotherms of the hierarchical CNT/Co₃O₄ microtubes at 77 K and (b) corresponding pore size distribution calculated using the BJH method. The surface area of the as-prepared materials is about 93.9 m² g⁻¹ with the pore sizes mostly below 15 nm.

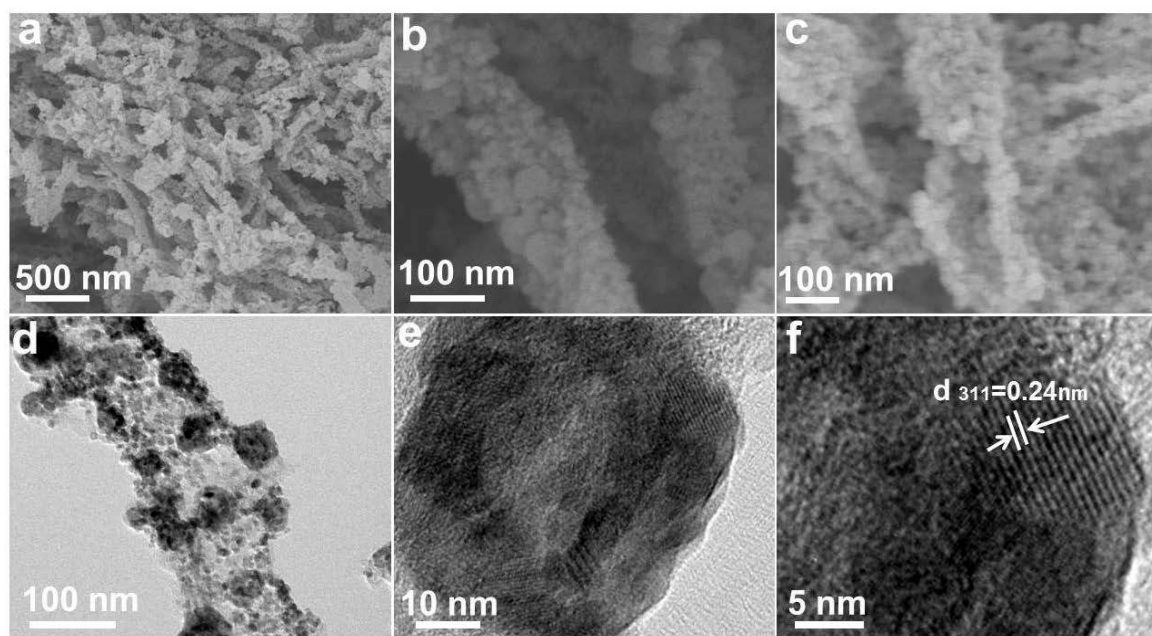


Figure S11. (a-c) FESEM, (d, e) TEM, and (f) HRTEM images of the synthesized Co₃O₄ microtubes.

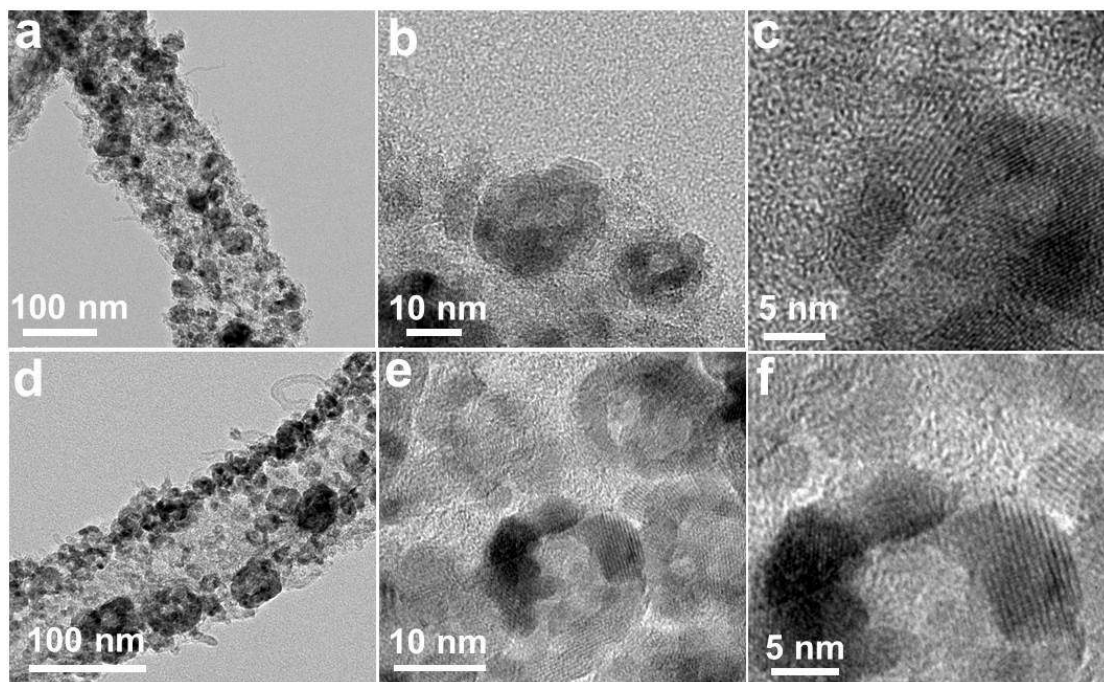


Figure S12. TEM and HRTEM images of the hierarchical CNT/Co₃O₄ microtubes heated in air at 340 °C (a-c) and 350 °C (d-f).

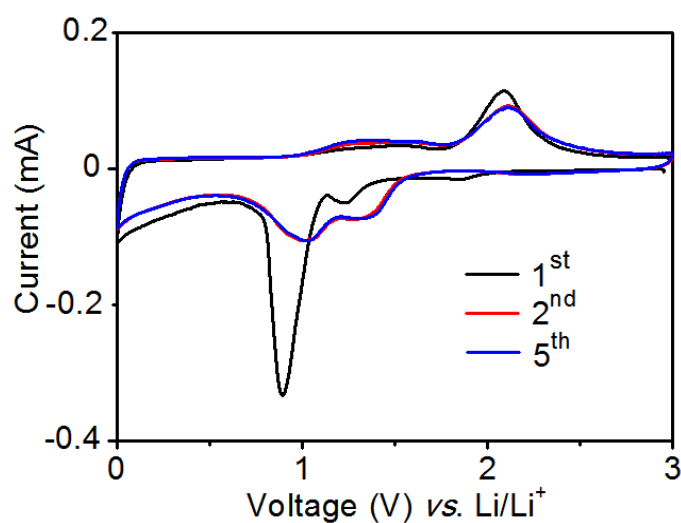


Figure S13. CV curves of the hierarchical CNT/Co₃O₄ microtube electrode. Since the oxidation states of cobalt in Co₃O₄ are Co³⁺ and Co²⁺, two cathodic peaks observed in the CV curves indicate the multi-step reaction behavior during the discharge process.

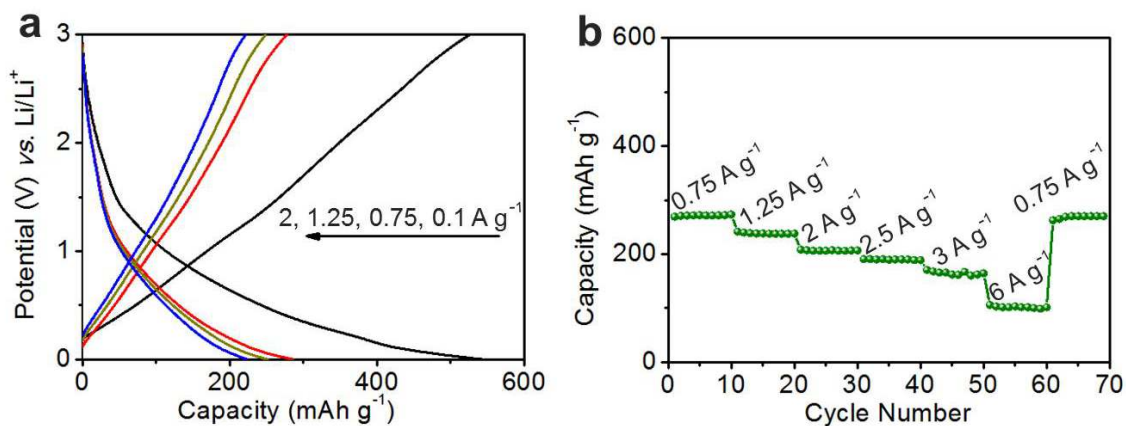


Figure S14. (a) Charge-discharge profiles and (b) rate performance of CNTs at different current densities. The employed CNTs are derived from the hierarchical CNT/Co₃O₄ microtubes after acid treatment (0.1 M HCl, treated at ambient temperature for 24h). The capacities of the CNTs are around 522, 274, 246, 219, 190, 165, and 102 mAh g⁻¹ at 0.1, 0.75, 1.25, 2, 2.5, 3, and 6 A g⁻¹, respectively, which are much lower than those of the hybrids. Therefore, the main capacity contribution for the composite is from the Co₃O₄ part.

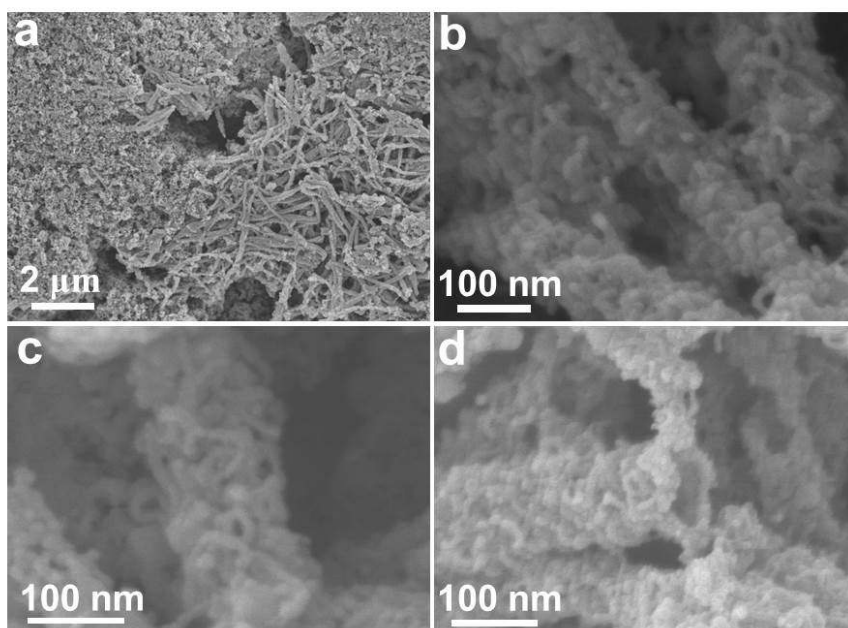


Figure S15. FESEM images of the hierarchical CNT/Co₃O₄ microtubes after 200 cycles.

Table S1. Comparison of lithium storage performance for the hierarchical CNT/Co₃O₄ microtubes with other Co₃O₄-based electrodes.

Material	Specific capacity	Cycle number	Mass loading	Ref.
CNT/Co ₃ O ₄ microtubes	1256 mAh g ⁻¹ at 0.1 A g ⁻¹ 771 mAh g ⁻¹ at 1 A g ⁻¹	200	~1 mg cm ⁻²	This work
Co ₃ O ₄ /carbon nanofibers (CNFs)	881 mAh g ⁻¹ at 0.05 A g ⁻¹	100	~1-2 mg cm ⁻²	[1]
Co ₃ O ₄ /carbon nanowires	534 mAh g ⁻¹ at 0.1 A g ⁻¹	20	Not reported	[2]
Porous Co ₃ O ₄ /CNFs	952 mAh g ⁻¹ at 0.1 A g ⁻¹ 750 mAh g ⁻¹ at 0.5 A g ⁻¹	100	~1 mg cm ⁻²	[3]
Co ₃ O ₄ /graphene	953 mAh g ⁻¹ at 0.05 A g ⁻¹	30	No reported	[4]
Co ₃ O ₄ /graphene	840 mAh g ⁻¹ at 0.1 A g ⁻¹	40	~2 mg cm ⁻²	[5]
Co ₃ O ₄ /CNTs	813 mAh g ⁻¹ at 0.1 A g ⁻¹ 514 mAh g ⁻¹ at 1 A g ⁻¹	100	No reported	[6]
Co ₃ O ₄ nanoparticles	800 mAh g ⁻¹ at 0.133 A g ⁻¹	15	No reported	[7]
Porous Co ₃ O ₄	686 mAh g ⁻¹ at 0.5 A g ⁻¹	60	No reported	[8]

Supplementary References

- [1] W. Yao, J. Yang, J. Wang, L. Tao, *Electrochim. Acta* **2008**, *53*, 7326.
- [2] P. Zhang, Z. P. Guo, Y. Huang, D. Jia, H. K. Liu, *J. Power Sources* **2011**, *196*, 6987.
- [3] S. Abouali, M. Akbari Garakani, B. Zhang, H. Luo, Z. L. Xu, J. Q. Huang, J. Huang, J. K. Kim, *J. Mater. Chem. A* **2014**, *2*, 16939.
- [4] Z. S. Wu, W. Ren, L. Wen, L. Gao, J. Zhao, Z. Chen, G. Zhou, F. Li, H. M. Cheng, *ACS Nano* **2010**, *4*, 3187.
- [5] D. Qiu, G. Bu, B. Zhao, Z. Lin, L. Pu, L. Pan, Y. Shi, *Mater. Lett.* **2014**, *119*, 12.
- [6] G. Huang, F. Zhang, X. Du, Y. Qin, D. Yin, L. Wang, *ACS Nano* **2015**, *9*, 1592.
- [7] R. Tummala, R. K. Guduru, P. S. Mohanty, *J. Power Sources* **2012**, *199*, 270.
- [8] C. Li, T. Chen, W. Xu, X. Lou, L. Pan, Q. Chen, B. Hu, *J. Mater. Chem. A* **2015**, *3*, 5585.